PAPER

Effect of hole transporting layers on the performance of PCPDTBT : PCBM organic solar cells

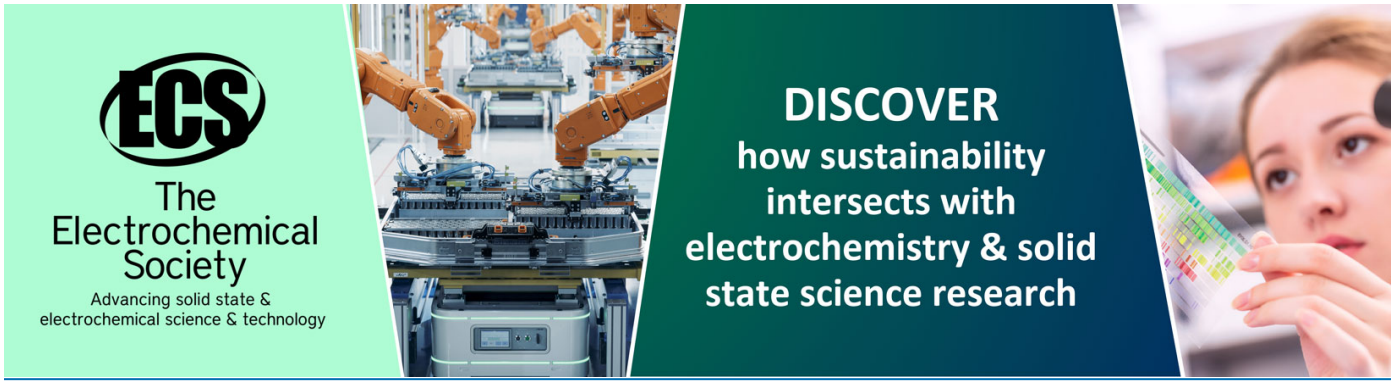

J. Phys. D: Appl. Phys. **45** (2012) 125102 (7pp) doi:10.1088/0022-3727/45/12/125102

Effect of hole transporting layers on the performance of PCPDTBT : PCBM organic solar cells

J Kettle[1], H Waters[1], M Horie[2] and S-W Chang[2]

[1] School of Electronic engineering, Bangor University, Dean st., Bangor, Gwynedd, LL57 1UT, Wales, UK
[2] Frontier Research Center on Fundamental and Applied Sciences of Matters, Department of Chemical Engineering, National Tsing-Hua University, 101, Sec. 2, Kuang-Fu Road, Hsin-Chu, 30013 Taiwan

Received 16 January 2012, in final form 10 February 2012
Published 6 March 2012
Online at stacks.iop.org/JPhysD/45/125102

Abstract
We study the performance of PCPDTBT : C_{71}-PCBM organic photovoltaics (OPVs) for three hole transporting layers (HTL); PEDOT : PSS, nickel oxide (NiO) and molybdenum trioxide (MoO_3). We show that devices fabricated with nickel oxide HTL demonstrate the highest power conversion efficiency and theoretical data using a transfer matrix model confirms that this is as a result of increased absorption in the active layer as well as a result of improved series resistance and improved matching of energy levels. Device degradation is studied and lifetime is highest for the NiO and MoO_3 based devices, proving that OPVs with this material system are less sensitive to the environmental effects of water, oxygen and irradiance.

(Some figures may appear in colour only in the online journal)

1. Introduction

Remarkable improvements in performance of organic photovoltaics (OPVs) have been made with bulk heterojunction (BHJ) devices, where organic polymers and fullerene derivatives are blended and then phase separated during coating to form nanoscale donor–acceptor interfaces [1, 2]. To demonstrate high efficiencies, the active layer of polymer solar cells must attain a high absorption of the solar spectrum. Therefore, one of the most critical challenges is to develop donor conjugated polymers that possess a low-energy band gap for strong and broad absorption spectrum extending to near-infrared to capture more solar photons, whilst simultaneously maintaining high hole mobility for efficient charge transport [3]. For this reason, low band gap donor conjugated polymers have been extensively designed, synthesized and tested for use in polymer solar cells in recent years. One promizing low band gap donor material is poly[(4,4-bis(2-ethylhexyl)-4*H*-cyclopenta [2,1-*b*; 3,4-*b*′] dithiophene-2,6-diyl-*alt*-2,1,3-benzothiadiazole-4,7-diyl], PCPDTBT, which has been proven to be one of the most efficient low band gap photovoltaic materials. For the PCPDTBT : C_{71}-PCBM based polymer solar cell, an efficiency of 5.5% has been achieved using morphological control with 1,8-octane-dithiol as an process additive [4, 5].

However, due to the large band offset between the work function of ITO and the highest occupied molecular orbital (HOMO) of PCPDTBT, recombination can occur at the interface, causing the photocurrent of the device to decrease. Therefore, to obtain high efficiency devices, a poly(3,4-ethylenedioxythiophene) : poly(styrenesulfonate) (PEDOT : PSS) layer is inserted between the opaque anode, ordinarily indium-tin oxide (ITO) and the active layer of the device [5, 6], to function as a hole transporting layer (HTL) and to limit the recombination at the interface of the active layer [7]. PEDOT : PSS is solution processible and possesses a suitable work function to act as an effective HTL, whilst maintaining high optical transparency in visible light and improving the smoothness of the interface between the anode and active layer [8]. Despite these perceived advantages, PEDOT : PSS can limit device performance in several ways. Firstly, the electrical properties can degrade with time and exposure to oxygen and water. Secondly, the lowest unoccupied molecular orbital (LUMO) of PEDOT : PSS is only approximately 0.6 eV above the LUMO of PCPDTBT, so electrons potentially diffuse into the PEDOT : PSS layer and recombine with holes, thereby decreasing device performance. Finally, In_2O_3 in ITO decomposes due to the strong acidic solution of PSS, which possesses a pH of 1.2 [9, 10]. For these reasons,

alternative HTLs based upon metal oxides such as p-type nickel oxide (NiO_x), vanadium (V) oxide (V_2O_5) and molybdenum trioxide (MoO_3) have been studied and OPV performance has demonstrated devices from these HTLs to have improved open-circuit voltage (V_{OC}), short-circuit current density (J_{SC}) and fill factor (FF) relative to a PEDOT : PSS control for poly (3-Hexylthiophene) (P3HT) : PCBM devices. NiO has also been demonstrated to be chemically stable and inert in relation to ITO and P3HT : PCBM and can be potentially applied by solution processing [11] onto flexible substrates.

Here, we report studies of optimizing HTLs in PCPDTBT : PCBM OPVs. We consider three HTLs; PEDOT : PSS and two metal oxide based HTLs including NiO_x, and MoO_3. Experimental data are used to optimize PEDOT : PSS thickness and NiO thickness. We use RF sputtered NiO and show that sputtered NiO coatings can act most effectively as HTLs in PCPDTBT : PCBM solar cells. Previous reports have shown that varying the HTL affects multiple characteristics of the OPV including the transport of holes to the anode [12], morphology of the active layer [8], absorption in the HTL [13] and light incoupling between the HTL and active layer [14]; these competing mechanisms together have a direct influence on device performance. In order to understand the differences in performances between the different HTLs, we demonstrate with optical modelling using a thin film multiple reflection (TFMR) that the increased photocurrent observed in thin metal oxide films is as a result of the increased average EM field across the active layer.

2. Experimental

Initially, samples are prepared onto ITO-coated glass (Psiotec Ltd, UK, $R_s = 16\,\Omega$/square), which are cleaned using deionized water, acetone and IPA in ultrasonic cleaner and blown dry using nitrogen. The samples are then placed into a UV ozone cleaner for 20 min.

For PEDOT : PSS tests only, a layer of PEDOT : PSS (HC Starck Clevios PAI 4083) was spin coated (in air) onto the substrate at various speed for 30 s before a 20 min bake at 120 °C on a hotplate to bake off any residual H_2O. Annealing temperature and time were kept at 120 °C and 20 min, respectively, for all experiments. Film thicknesses were measured using a Veeco Dektak. For the metal oxide HTL tests, deposition is undertaken using the experimental section 2.2.

Blends of donor/acceptor material (ratio 1 : 3) were prepared with a concentration of 30 mg mL^{-1} in anhydrous chlorobenzene with 10 mg mL^{-1} of 1,8-octanedithiol. Donor material, PCPDTBT ($M_n = 40\,600$, $M_w/M_n = 2.44$), was synthesized by palladium catalysed Suzuki coupling polymerization using a similar procedure discussed in a previous paper [15]. Acceptor material, C_{71}-PCBM, was supplied by Nano-C. Devices were fabricated in a glovebox, which maintains H_2O and O_2 concentrations below 1 part per million. The active layer consisting of a donor/acceptor blend was applied by spin coating inside the glovebox using 2500 rpm for 60 s, which produces a film thickness of 110 nm. Thermal evaporation of the cathode was performed through a shadow mask to define device area and consisted of 2 nm lithium fluoride (LiF) and 80 nm of aluminium (Al). The chamber was pumped to 5×10^{-7} mBar and kept below 2×10^{-6} mBar during the evaporation. The measurement system used to characterize the devices consisted of a Newport solar simulator with AM1.5 output, which was calibrated using a silicon reference cell verified by RERA. All measurements were carried out with a minimum of 10 devices using a Botest GmbH measurement unit.

Lifetime measurements were undertaken with constant exposure to AM1.5G conditions, following ISOS-L-1 procedures as discussed outlined by Reese *et al* [16]. The devices were measured without encapsulation and in ambient air, in order to accelerate the degradation. Humidity and temperature were uncontrolled but measured at 45% and 18 °C, respectively. Parameters were extracted from J–V characteristics, which were taken at various intervals across a 500 h period.

2.1. Thermal evaporation

For MoO_3 films, thermal evaporation was undertaken from a quartz crucible. The pressure was also kept under 8×10^{-7} mbar during the deposition, using a rate of 0.1 nm per second. No post-treatment was undertaken for MoO_3 HTLs. No further thermal annealing was used. Attempts were made to fabricate devices with thermally evaporated V_2O_5 and thermally evaporated NiO_x but devices exhibited poor FF, so are not discussed in this paper.

2.2. Nickel oxide sputter deposition

Sputtered nickel oxide (NiO_x) thin films were prepared by RF magnetron sputtering using a NiO target (3″ diameter, 99.99% purity) at a working pressure of 1×10^{-2} mbar using an argon and oxygen gas mixture (55–45%) directly onto ITO-coated covered glass. The target–substrate separation was rotated and kept at 5 cm from the sputter target. The films were prepared on unheated substrates with an RF power of 100 W. No post-deposition plasma treatment or thermal annealing was used. Thicknesses of both the MoO_3 and the NiO_x layers were tooled for a range of three different thicknesses using a Dektak profilometer.

2.3. Modelling of the optical absorption in active layer

In order to understand the differences in measured OPV performance between PCPDTBT : PCBM OPVs fabricated with the different HTLs, optical modelling has been undertaken. Several attempts have been made to model the optical performance in OPVs and relate that to the generated photocurrent and power conversion efficiency using simple TFMR models [17–19]. This technique calculates transmission, reflection at each interface and interference in a multi-layer system and the absorption profile across each layer, whose structure is shown in figures 1(*a*)–(*b*). Time-averaged energy dissipation at the point z can be calculated from the absorption coefficient and electromagnetic field intensity and then the accumulated dissipation can be

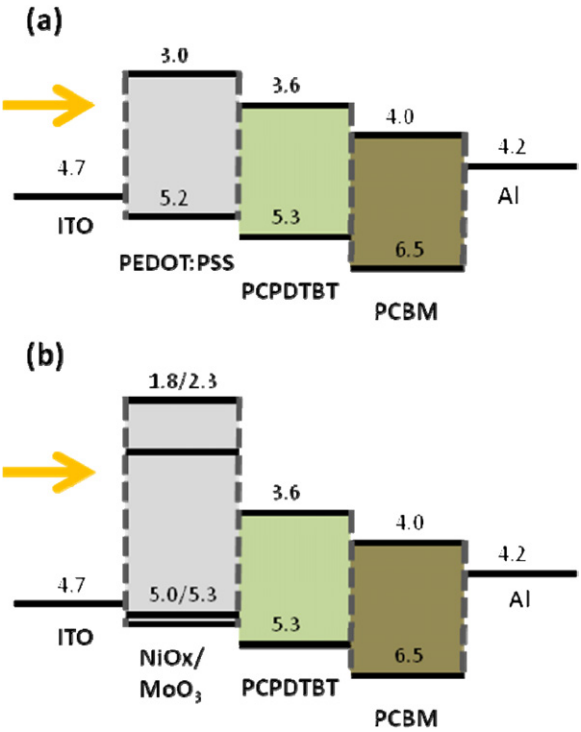

Figure 1. Ideal flat band energy diagram for a PCPDTBT : PCBM solar cell with (*a*) PEDOT : PSS and (*b*) NiO ($E_V = 5.3$ eV, $E_C = 1.8$ eV)/MoO_3 ($E_V = 5.0$ eV, $E_C = 2.3$ eV) HTLs. Light is incident from the ITO side of the device, therefore the HTL needs to remain opaque in the absorption spectrum of PCPDTBT : PCBM.

calculated for obtaining the exciton generation. An integral of the accumulated dissipated energy as a function of wavelength and intensity is implemented in order to model for illumination under AM1.5G conditions. Data for the complex refractive index ($\tilde{n} = n + i\kappa$) were obtained experimentally using elipsometry for the materials and compositions described in the experimental using a J.A. Woolam WVASE elipsometer. By assuming that the internal quantum efficiency is 100%, it is possible to derive expressions for the maximum short-circuit current density, $J_{SC\text{-}MAX}$. Whilst the model does not account for recombination at the HTL interfaces after electron–hole separation, it gives a figure of merit for differences in absorption of light in the active layer for different hole transport layers.

3. Results

3.1. Effect of PEDOT : PSS thickness

Data in figures 2(*a*)–(*d*) show the performance of a PCPDTBT-PCBM OPV as a function of PEDOT : PSS thickness, with data summarized in table 1. PEDOT : PSS is the most commonly used HTL for PCPDTBT-PCBM solar cells; however, there are few reports on the optimization of this layer and the effect upon device performance. Devices with PEDOT : PSS thicknesses varying between 30 and 130 nm were compared with the active layer processing and thickness kept constant. A control device (fabricated on bare-ITO) is shown in figure 2, demonstrating the performance decrease observed in PCPDTBT : PCBM without the use of a HTL. Apart from the ITO-PCPDTBT : PCBM device, only a minor variance in open-circuit voltage (V_{OC}) is observed over the range of PEDOT : PSS layer thicknesses (14 mV). Device performance is relatively sensitive to PEDOT : PSS film thicknesses over the range measured (30–130 nm) and optimal device performance is found using the thinner PEDOT : PSS layers (optimal thickness = 41 nm) as a result of increased absorption in the active layer, which is supported by the increase in short-circuit current density (J_{SC}) with reduced PEDOT : PSS thickness. FF is shown to have only a minor dependence upon film thickness (∼4% decrease in relative performance with thinner layers compared with thicker layers). The relatively minor reduction in FF is dwarfed by the more significant increase in J_{SC}, which is found to increase with thinner layers (∼13% reduction in relative performance), causing an increase to PCE.

Optical modelling confirms that for thinner PEDOT : PSS layers, the electric field modulation, and thus absorption, within the active layer is greater. Strong interference effects between the incident light and the light reflected from the Al cathode give rise to interference maxima and minima, which are shown using modelling to vary with PEDOT : PSS thickness. Figure 3(*a*) shows the electric field intensity ($|E^2|$) across an OPV with a 41 nm thick layer and for 3(*b*) 130 nm PEDOT : PSS layer and the peak of $|E^2|$ is shown to be much greater in the active layer when using 41 nm of PEDOT : PSS. Therefore, modelled $J_{SC\text{-}MAX}$ values are calculated at 15.70 mA cm^{-2} for the 41 nm PEDOT : PSS layer and (*b*) 14.11 mA cm^{-2} for the 130 nm PEDOT : PSS layer, which corresponds to a relative decrease of 12%, in excellent correlation with the experimental results. In general, the trend observed shows that as thickness of the PEDOT : PSS layer is increased, the total absorbed light in the active layer decreases due to the main maxima peak shifting towards the thick PEDOT : PSS layer and the main minima peak shifting towards the active layer. This is more pronounced for $\lambda = 750$ nm, where PCPDTBT : PCBM films are strongly absorbing. The one exception to this trend of increasing PCE values with decreased PEDOT : PSS layers is for experimental data at the lower thickness PEDOT : PSS (<34 nm). AFM data indicate that the surface roughness increases at the thinner layers, which almost certainly has an adverse effect upon the active layer morphology (For 30 nm PEDOT : PSS, $R_A = 0.288$ nm, $R_Z = 4.17$ nm, for 41 nm PEDOT : PSS, $R_A = 0.195$ nm, $R_Z = 3.05$ nm). The experimental data appear to show a relatively minor reduction in the series resistance (R_S) as layer thickness is varied (5% relative change), so whilst this contributes, the data suggest this is only a relatively minor contribution.

3.2. Effect of NiO and MoO_3 thickness upon OPV performance

Data in figures 2(*a*)–(*d*) also show the effect of film thickness on the performance of PCPDTBT : PCBM OPVs for sputtered (NiO) nickel oxide and MoO_3 HTLs, with data summarized in table 2. Generally, as absorption is much higher in metal oxide based HTLs, thin layers are used [11, 13, 20]. As with devices

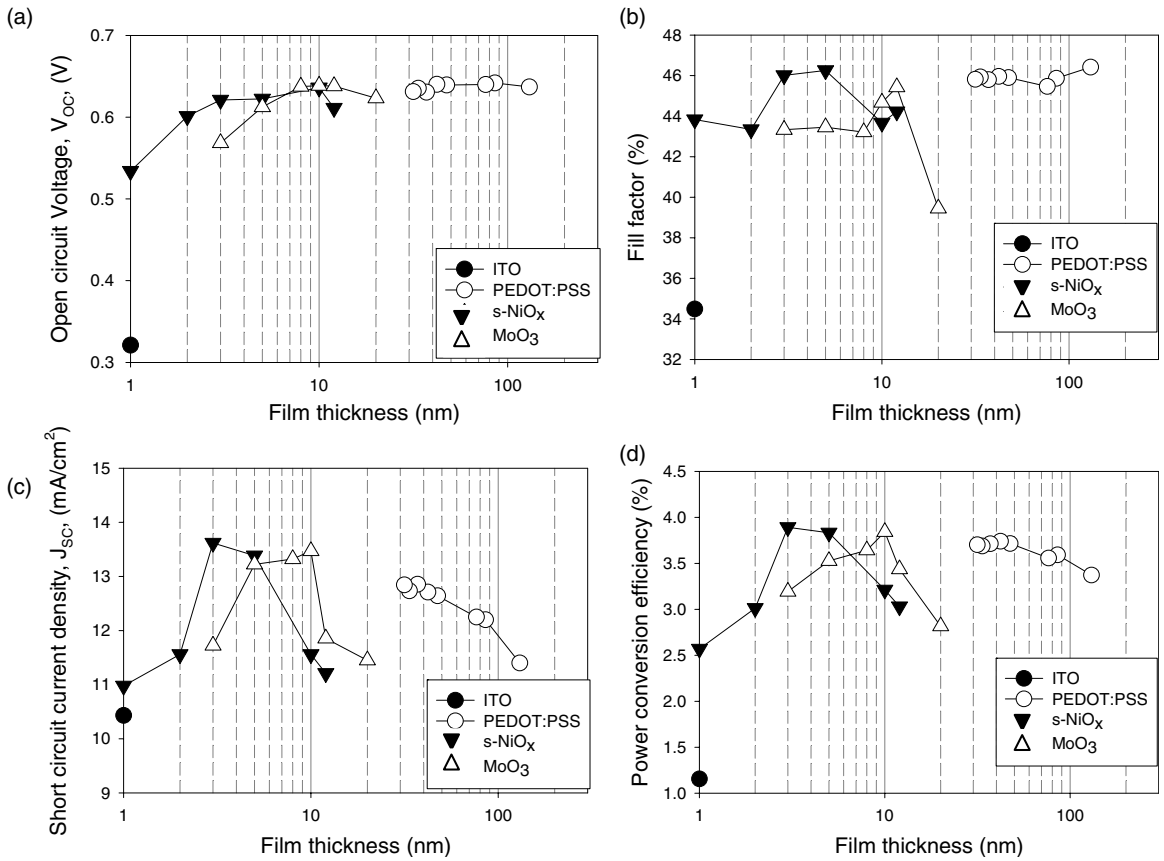

Figure 2. Effect of HTL thickness on PCPDTBT : PCBM for PEDOT : PSS, NiO and MoO_3 films upon (*a*) V_{OC}, (*b*) FF, (*c*) J_{SC} and (*d*) PCE. Please note logarithmic scale for the film thickness.

Table 1. Summary of OPV results for different thickness PEDOT : PSS HTLs under AM1.5G conditions. The standard deviation for the PCE is shown in brackets in the PCE column.

PEDOT : PSS thickness (nm)	V_{OC} (V)	J_{SC} (mA cm^{-2})	FF	PCE (%)
31.55	0.6321	12.80	45.81	3.70 (0.0112)
33.56	0.6305	12.74	45.93	3.69 (0.0181)
37.1	0.6305	12.87	45.8	3.71 (0.0131)
42.11	0.6402	12.71	45.96	3.74 (0.0131)
47.45	0.6394	12.65	45.93	3.72 (0.0120)
76.45	0.6399	12.22	45.47	3.58 (0.0147)
85.44	0.6419	12.20	45.87	3.59 (0.0176)
130.223	0.6374	11.40	46.41	3.37 (0.0146)

fabricated with the PEDOT : PSS active layer, the thickness and process conditions of the active layer were kept constant. For all HTLs, the PCE was found to increase by insertion of the HTL layer, under optimized conditions, when compared with a device on bare ITO. The maximum PCE of 3.89% was obtained with the 3 nm thick NiO layer. It is worth noting this PCE lower than previous reports [5, 15], but the results in this paper use larger device areas (device area = 0.2 cm^2).

As with previous reports [11, 13, 20], there is a trend of optimal thicknesses of metal oxide HTLs and OPV performance is very sensitive to film thickness in the range investigated. Considering the NiO film only, when the HTL film thickness is less than 3 nm, PCE remains low (<3%). AFM scans indicate that the substrate is covered with isolated islands of NiO and not a continuous film; therefore, the NiO acts as only a partial HTL to the PCPDTBT donor polymer, resulting in higher recombination of electrons with holes at the anode, causing reduced hole transport between the anode and active layer and lower V_{OC}. As NiO thickness increases, the film becomes continuous and PCE peaks at approximately 3 nm thickness. PCE then declines with NiO thicknesses >6 nm, which is as a result of increased series resistance and partly as a result of a small increase in absorption in the NiO film, which is confirmed by the drop in the measured J_{SC} of the device. The FF measurement was observed to initially increase from 34.5% (bare ITO) to 46.3% as NiO was increased to 3 nm and then remained relatively constant for thicknesses up to 10 nm. A similar trend is also observed for the MoO_3 devices with an optimal thickness measured at 8 nm instead. V_{OC} initially increases with film thickness to 0.64 V and remains constant thereafter. FF and J_{SC} initially increase from low value and reach a peak at a thickness of 10 nm. The decrease in performance seems to be only as a result of series resistance increase.

3.3. Comparison of NiO/MoO_3 and PEDOT : PSS hole transport layers

Figure 4 shows the current density–voltage (J–V) characteristics of PCPDTBT : PCBM devices with the optimized PEDOT : PSS, NiO and MoO_3 HTLs. For comparison, the J–V characteristics corresponding to a device fabricated onto

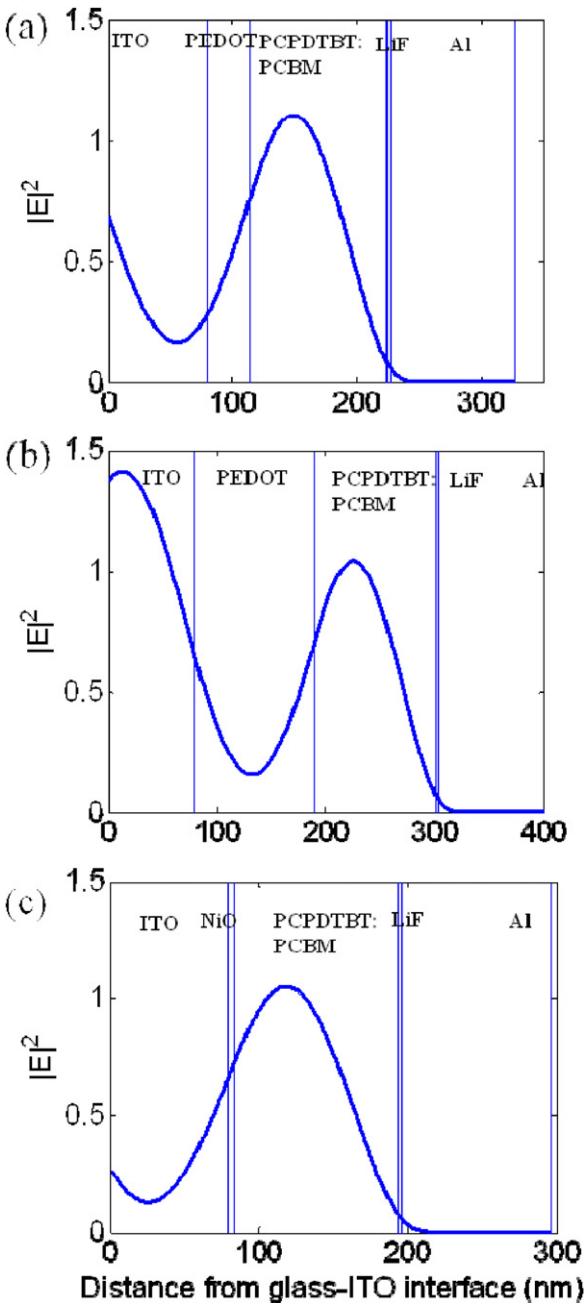

Figure 3. Electric field intensity for ITO-HTL-PCPDTBT-LiF-AL devices where the HTL is (*a*) 41 nm PEDOT : PSS (*b*) 130 nm PEDOT : PSS and (*c*) 3 nm s-NiO and incident wavelengths of 750 nm. The calculated $J_{SC\text{-}MAX}$ for each device are shown as an inset to each figure is (*a*) 16.70 mA cm^{-2}, (*b*) 14.11 mA cm^{-2} and (*c*) 17.13 mA cm^{-2}. Light is incident from the left-hand side of the schematic.

bare-ITO is shown. It is apparent that irrespective of the HTL type, OPV device performance is enhanced with the addition of a HTL, which is attributed to the improved efficiency of hole transfer between PCPDTBT and the different HTLs and reduced recombination at the anode.

The NiO device outperforms the PEDOT : PSS; primarily as a result of increased J_{SC}, despite a small reduction in V_{OC}. The MoO_3 demonstrates slightly improved performance over the PEDOT : PSS layer; the J_{SC} of the MoO_3 device

Table 2. Summary of results for optimized HTLs under AM1.5G conditions. The standard deviation for the PCE is shown in brackets in the PCE column.

HTL properties	V_{OC} (V)	J_{SC} (mA cm^{-2})	FF	PCE (%)	R_S (Ω cm^2)
ITO-only	0.321	10.43	34.49	1.17 (0.042)	15.99
PEDOT : PSS (42 nm)	0.640	12.71	45.97	3.74 (0.0121)	13.37
s-NiO (3 nm)	0.621	13.62	46.01	3.89 (0.0283)	10.47
MoO_3 (10 nm)	0.631	13.46	44.67	3.84 (0.0198)	12.27

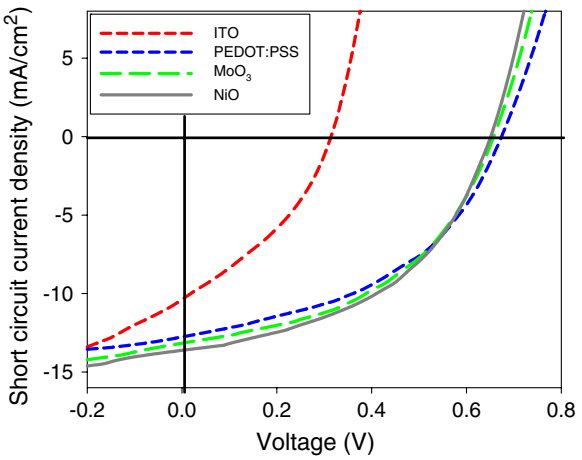

Figure 4. Optimized J–V characteristics under AM1.5G conditions for the s-NiO, MoO_3 and PEDOT : PSS HTLs with a comparison to a control device without a HTL.

is higher, but the FF is less, suggesting some reduction in charge extraction, probably as a result of the rougher interface morphology. The standard deviation of the measurements are shown in table 2. The other noticeable trend from the standard deviations is that the PEDOT : PSS devices exhibited lower variations in performance than the NiO or MoO_3 devices.

In order to understand the differences in performance between the PEDOT : PSS layer and NiO layer, data for electric field intensity ($|E^2|$)as a function of position, z, in the plane of incident light are shown in figure 3(*a*) for a 41 nm PEDOT : PSS and (*c*) 3 nm NiO HTL. Data are shown for a single of 750 nm, as the absorption spectrum of PCPDTBT : PCBM has a main absorption wavelength at approximately 750 nm. $J_{SC\text{-}MAX}$ values calculated at (a) 16.50 for the 30 nm PEDOT : PSS layer and (c) 17.23 mA cm^{-2} for the NiO layer, which represents only a ~4% relative difference in photocurrent. However, the drop in experimentally measured PCE by changing the HTL is by contrast much larger (~16% relative drop in PCE), indicating that the likely improvement in performance when switching from a PEDOT : PSS to NiO HTL is not as a result of differences in electric field modulation alone.

This difference can be explained by two factors; firstly NiO is better aligned to the energy levels of PCPDTBT [20]. The optical band gap of NiO is around 3.2 eV and for MoO_3 around 3.0 eV, with the conduction band at around 1.8 eV and 2.3 eV, respectively, with the LUMO of PCPDTBT at around 3.6 eV [21] and around 4.0 eV for C_{70}-PCBM; this should give a potential barrier of around 1.8 eV or 1.3 eV to electrons at the

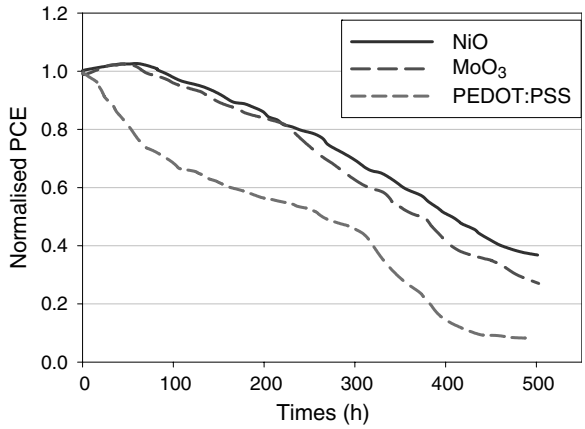

Figure 5. Variations of the PCE of devices submitted to continuous illumination over 500 h. Samples with a stack of ITO-PEDOT : PSS-PCPDTBT/PCBM-LiF-Al degraded quicker than devices with the same structure but a NiO or MoO_3 HTL.

anode in PCPDTBT and around 2.4 eV and 1.7 eV for electrons at the anode in C_{70}-PCBM for NiO and MoO_3, respectively. This compares with a potential barrier of around 0.6 eV and 1.0 eV to a PEDOT : PSS HTL. This suggests that using NiO or MoO_3 layers, rather than PEDOT : PSS, would act as improved HTL with reduced recombination of holes before extraction into the electrodes, which is reflected in the slightly improved FF measurements of the optimized devices. Secondly, the series resistance of the device fabricated with NiO and MoO_3 HTLs is reduced when compared with PEDOT : PSS devices (a relative decrease of 27% and 17%, respectively). Therefore, NiO layers should be preferred for HTLs not just because of increased electric field modulation in the active region, but also because the energy levels are better aligned to PCPDTBT and reduced the series resistance of devices.

3.4. Lifetime measurements

For optimized devices reported in table 2, lifetime measurements of devices were conducted. Measurements were taken with non-encapsulated devices to accelerate the testing. Figure 5 shows the normalized PCE performance over a 500 h time span. It is apparent that the performance of the device fabricated with PEDOT : PSS degraded at a faster rate than that of the MoO_3 or NiO devices, in good correlation with other reports of NiO layers in P3HT : PCBM devices [11, 20]. Studies on the degradation of other material systems have concluded that PEDOT : PSS can increase in resistance due to the uptake of atmospheric water and react with the ITO electrode due to the acidic nature of PSS and inevitably this degradation is apparent also in PCPDTBT : PCBM cells.

For the NiO and MoO_3 devices, PCE is seen to actually increase in the first 80 h of operation. This increase is not witnessed in the PEDOT : PSS device owing to the rapid initial decrease in performance. Further tests are ongoing to study the effect of degradation in PCPDTBT-based solar cells; however, the data in figure 5 show that OPV lifetime in PCPTBT : PCBM cells enhanced the substitution of the HTL from PEDOT : PSS to NiO or MoO_3. Devices still exhibited relatively short lifetimes compared with other PV systems, however, for these experiments; all devices were fabricated using LiF/Al cathode contacts. It is likely that this is a major source of degradation in these devices due to Li+ diffusion; therefore lifetimes could be further enhanced with alteration of the electron transporting layer (ETL) and cathode and replacing the LiF with calcium [22].

4. Conclusions

This paper looks at optimizing the HTLs for PCPDTBT : PCBM solar cells. Both polymeric and metal oxide HTLs have been studied and the best performing HTL has been shown to be a 3 nm sputtered NiO layer. Furthermore, the stability of OPVs fabricated with a NiO layer was enhanced by removing the PEDOT : PSS HTL. The reason for this performance increase was a combination of factors; better alignment of the energy levels, improved series resistance and also an increase in electric field across the active region. For PEDOT : PSS layers, improved performance is observed with thinner layers, as a result of the increased modulation of the electric field within the active region, with only a minor improvement in series resistance observed; however, a limit appears to be reached when the thickness is reduced to below 34 nm.

Acknowledgments

The authors would like to thank the Royal Society, London, for their support through the Research grant scheme. Additionally, we would like to thank Dr Yanhua Hong for her assistance with the AFM results. HW would like to thank Bangor University for the 125 scholarship.

References

[1] Scharber M C, Mühlbacher D, Koppe M, Denk P, Waldauf C, Heeger A J and Brabec C J 2006 *Adv. Mater.* **18** 789–94
[2] Heum Park S, Roy A, Beaupré S, Cho S, Coates N, Moon J S, Moses D, Leclerc M, Lee K and Heeger A J 2009 *Nature Photon.* **3** 297–302
[3] Mondal R, Ko S, Norton J E, Miyaki N, Becerril H A, Verploegen E, Toney M F, Brédas J-L, McGehee M D and Bao Z 2009 *J. Mater. Chem.* **19** 7195–7
[4] Lee J K, Ma W L, Brabec C J, Yuen J, Moon J S, Kim J Y, Lee K, Bazan G C and Heeger A J 2008 *J. Am. Chem. Soc.* **130** 3619–23
[5] Peet J, Kim J Y, Coates N E, Ma W L, Moses D, Heeger A J and Bazan G C 2007 *Nature Mater.* **6** 497–500
[6] Yu G, Gao J, Hummelen J C, Wudl F and Heeger A J 1995 *Science* **270** 1789–91
[7] Cravino A, Schilinsky P and Brabec C J 2007 *Adv. Funct. Mater.* **17** 3906–10
[8] Kim Y, Ballantyne A M, Nelson J and Bradley D C 2009 *Org. Electron.* **10** 205–9
[9] Hains A W and Marks T J 2008 *Appl. Phys. Lett.* **92** 23504–6
[10] de Jong M P, van Ijzendoorn L J and de Voigt M J A 2000 *Appl. Phys. Lett.* **77** 2255–7
[11] Sun N, Fang G, Qin P, Zheng Q, Wang M, Fan X, Cheng F, Wan J, Zhao X, Liu J, Carroll D L and Ye J 2010 *J. Phys. D: Appl. Phys.* **43** 445101
[12] Shrotriya V, Li G, Yao Y, Chu C-W and Yang Y 2006 *Appl. Phys. Lett.* **88** 73508–10

[13] Betancur R, Maymó M, Elias X, Vuong L T and Martorell J 2011 *Sol. Energy. Mater. Sol. Cells* **95** 735–9
[14] Park S-Y, Kim H-R, Kang Y-J, Kim D-H and Kang J-W 2010 *Solar Energy Mater. Sol. Cells* **94** 2332–6
[15] Kettle J, Horie M, Majewski L A, Saunders B R, Tuladhar S, Nelson J and Turner M L 2011 *Sol. Energy Mater. Sol. Cells* **95** 2186–93
[16] Reese M O *et al* 2011 *Sol. Energy Mater. Sol. Cells* **95** 1253–67
[17] Pettersson L A A, Roman L S and Inganas O 1999 *J. Appl. Phys.* **86** 487–97
[18] Burkhard G F , Hoke E T and McGehee M D 2010 *Adv. Mater.* **22** 3293–3297
[19] Boland P, Lee K, Dean J and Namkoon G 2010 *Sol. Energy. Mater. Sol. Cells* **94** 2170–5
[20] Irwin M D, Buchholz D B, Hains A W, Chang R P H and Marks T J 2008 *Proc. Natl Acad. Sci. USA* **105** 2783–7
[21] Morana M, Wegscheider M, Bonanni A, Kopidakis N, Shaheen S, Scharber M, Zhu Z, Waller D, Gaudiana R and Brabec C 2008 *Adv. Funct. Mater.* **18** 1757–66
[22] de Bettignies R, Leroy J, Firon M and Sentein C 2006 *Synth. Met.* **156** 510–3